ELSEVIER

Materials Science and Engineering C 16 (2001) 3–10

MATERIALS SCIENCE & ENGINEERING C

www.elsevier.com/locate/msec

Mechanical and electrostatic properties of carbon nanotubes and nanowires

Z.L. Wang [a,*], R.P. Gao [a,b], P. Poncharal [c], W.A. de Heer [c], Z.R. Dai [a], Z.W. Pan [a]

[a] *School of Materials Science and Engineering, Georgia Institute of Technology, Atlanta, GA 30332-0245, USA*
[b] *University of Science and Technology Beijing, Beijing, People's Republic of China*
[c] *School of Physics, Georgia Institute of Technology, Atlanta, GA 30332-0245, USA*

Abstract

Nano-scale manipulation and property measurements of individual nanowire-like structure is challenged by the small size of the structure. Scanning probe microscopy has been the dominant tool for property characterizations of nanomaterials. We have developed an alternative novel approach that allows a direct measurement of the mechanical and electrical properties of individual nanowire-like structures by in situ transmission electron microscopy (TEM). The technique is unique in a way that it can directly correlate the atomic-scale microstructure of the nanowire with its physical properties. This paper reviews our current progress in applying the technique in investigating the mechanical and electron field emission properties of carbon nanotubes and nanowires.

Keywords: Carbon nanotubes; Nanowires; Emission properties

1. Introduction

Applications of nanomaterials in nanotechnology are facing four main challenges: material preparation, property characterization, device fabrication and system integration. Due to the high size and structure diversity of nanomaterials, their physical properties strongly depend on their atomic-scale structure, size and chemistry [1]. To fully utilize the basic and technological advantages offered by the size specificity and selectivity of the nanomaterials, it is essential to investigate the unique characteristics of individual nanomaterials, such as a single carbon nanotube or nanowire with well understood microstructures.

Scanning probe microscopy (STM, AFM) has been a powerful tool in manipulating and characterizing the properties of individual nanostructures. This is the dominant approach towards nanomanipulation. Transmission electron microscopy on the other hand, has been traditionally applied to characterizing the intrinsic structures of nanomaterials. We have recently developed in situ transmission electron microscopy (TEM) as a novel approach for measuring the properties of individual wire-like structures [2–4]. This is a new technique that can not only provide the properties of an individual nanowire but can also give the structure of the nanowire through electron imaging and diffraction, providing an ideal technique for understanding the one-to-one property–structure relationship.

In this paper, our current progress in applying in situ TEM for property nanomeasurements is reviewed. We will concentrate on the mechanical properties of nanowire-like structures and the electron field emission induced structural change in carbon nanotubes.

2. Experimental results

2.1. Bending modulus of carbon nanotubes produced by arc-discharge

It is known that TEM is a powerful tool for studying the intrinsic microstructure of materials. To use TEM for property nanomeasurements, its specimen stage must be modified to allow applying an electric field across the sample. The static and dynamic properties of the nanotubes can be obtained by applying a controllable static and alternating electric field. Our experiments were carried out using a JEOL 100C TEM (100 kV), as reported in details elsewhere [4]. An oscillating voltage with tunable frequency was applied on the nanotubes. Mechanical reso-

* Corresponding author. Tel.: +1-404-894-8008; fax: +1-404-894-9140.
E-mail address: zhong.wang@mse.gatech.edu (Z.L. Wang).

0928-4931/01/$ - see front matter
PII: S0928-4931(01)00293-4

nance can be induced in carbon nanotubes if the applied frequency approaches the resonance frequency (Fig. 1). Theoretically, resonance is nanotube selective because the natural vibration frequency depends on the tube outer diameter (D), inner diameter (D_1), the length (L), the density (ρ), and the bending modulus (E_b) of the nanotube [5],

$$f_i = \frac{\beta_i^2}{8\pi}\frac{1}{L^2}\sqrt{\frac{\left(D^2 + D_1^2\right)E_\beta}{\rho}} \quad (1)$$

where $\beta_1 = 1.875$ and $\beta_1 = 4.694$ for the first and the second harmonics. If the parameters D, D_1 and L can be provided by TEM images, the density ρ is known, the bending modulus E_b can be directly derived from the observed resonance frequency. This is the principle of our experiments.

To apply Eq. (1) for data analysis, it is vital to identify the true fundamental frequency. In practical experiments, carbon nanotubes are positioned against a counter electrode. Because of the difference between the surface work functions between the carbon nanotube and the counter electrode (such as Au), a static charge exists to balance this potential difference even at zero applied voltage. Therefore, under an applied field, the induced charge on the carbon nanotube can be represented by $Q = Q_o + \alpha V_d \cos 2\pi ft$, where Q_o represents the charge on the tip to balance the difference in surface work functions, α is a geometrical factor, and V_d is the amplitude of the applied voltage. The force acting on the carbon nanotube is:

$$F = \beta(Q_o + \alpha V_d \cos 2\pi ft)^2 = \left[\beta Q_o^2 + \alpha^2 \beta V_d^2/2\right] + 2\alpha\beta Q_o V_d \cos 2\pi ft + \alpha^2\beta V_d^2/2\cos 4\pi ft, \quad (2)$$

where β is a proportional constant. Thus, resonance can be induced at f and $2f$ with vibration amplitudes proportional to V_d and V_d^2, respectively. The former is a linear term in which the resonance frequency equals to the applied frequency, while the latter is a nonlinear term and the resonance frequency is twice of the applied frequency. There are two ways to determine the fundamental frequency. For the linear term, the vibration amplitude is linearly dependent on the magnitude of the voltage V_d (Fig. 2). Alternatively, one needs to examine the resonance at a frequency that is half or close to half of the observed resonance frequency to ensure no resonance occurring. The latter is the most convenient technique used in practice.

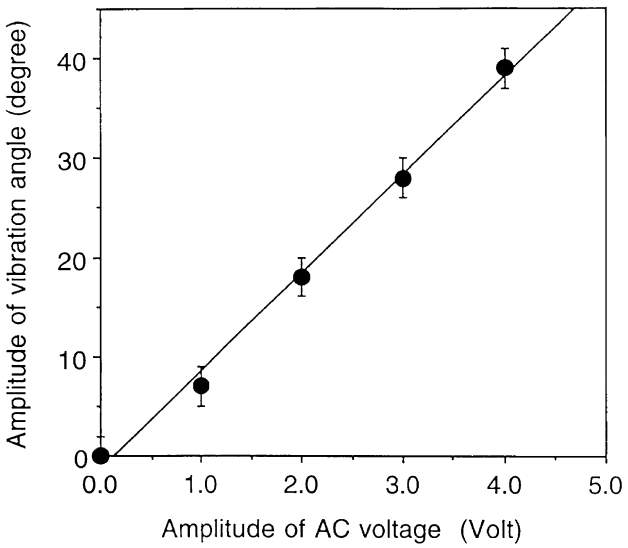

Fig. 2. Experimentally measured full vibration angle of a carbon nanotube as a function of the amplitude of the applied AC voltage.

The FWHM of the resonance peak of a carbon nanotube was determined by observing the dependence of the vibration amplitude on the frequency of the applied electric field, as shown in Fig. 1c. The ratio between the FWHM to the resonance frequency is $\Delta\nu/\nu_1 = 0.6$–0.7%. This value remains the same for several carbon nanotubes of dis-

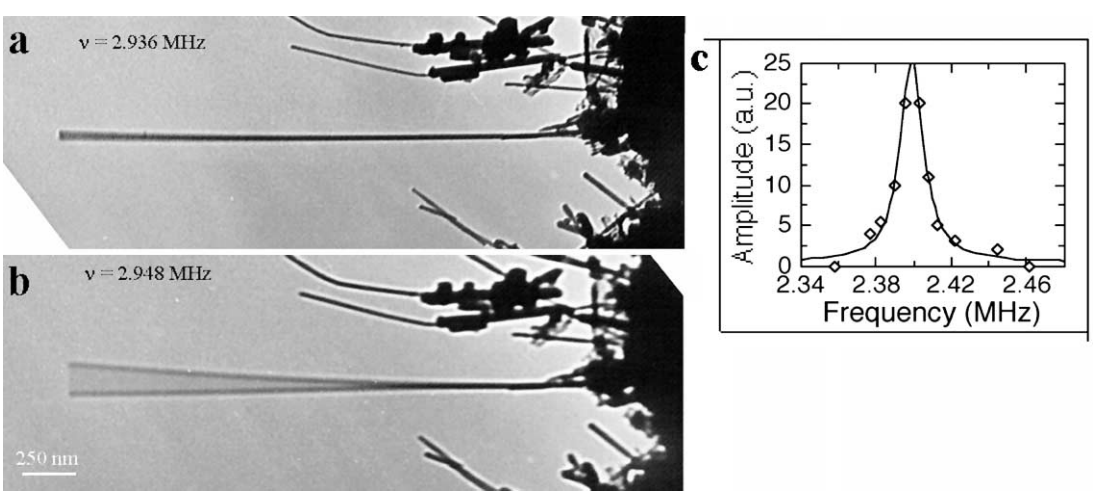

Fig. 1. A carbon nanotube produced by arc-discharge at (a) off-resonance and (b) on-resonance by varying the frequency of the externally applied electric field. (c) The full width at half maximum of the resonance peak.

Fig. 3. A bent carbon nanotube at (a) stationary, (b) the first and (c) the second harmonic resonance induced by an externally applied electric field.

tinctly different structures. This suggests that the viscosity coefficient of the nanotube in the conventional vacuum is almost independent of the intrinsic structure of the nanotubes.

Our first group of experiments was carried out for carbon nanotubes produced by an arc-discharge technique. The carbon nanotubes have diameters 5–50 nm and lengths of 1–20 μm and most of them are nearly defect-free. After a systematic study of the multiwalled carbon nanotubes, the bending modulus of the nanotubes was measured as a function of their diameters [2]. The bending modulus is as high as 1.2 TPa (as strong as diamond) for nanotubes with diameters smaller than 8 nm, and it drops to as low as 0.2 TPa for those with diameters larger than 30 nm. A decrease in bending modulus as the increase of the tube diameter is attributed to the wrinkling effect of the wall of the nanotube during small bending. This effect almost vanishes when the diameters of the tubes are less than 12 nm.

Carbon nanotubes may suffer from mechanical deformation so that their shape may not be perfectly straight. Fig. 3b,c shows the first and second harmonic resonance of a bent carbon nanotube, respectively. It appears that the resonance occurs in the plane parallel to the bending plane. The mechanical property of the nanotube can still be derived if the geometry of the nanotube is considered in the theoretical calculation.

For an anisotropy nanowire, there could exist two fundamental frequencies due to the difference in moments of inertia about the two axes perpendicular to the nanotube. Fig. 4 shows such a case, in which a small difference is noticed between the two resonance directions. This experiment apparently demonstrates that the anisotropy effect in nanowire structure can be measured experimentally through resonance.

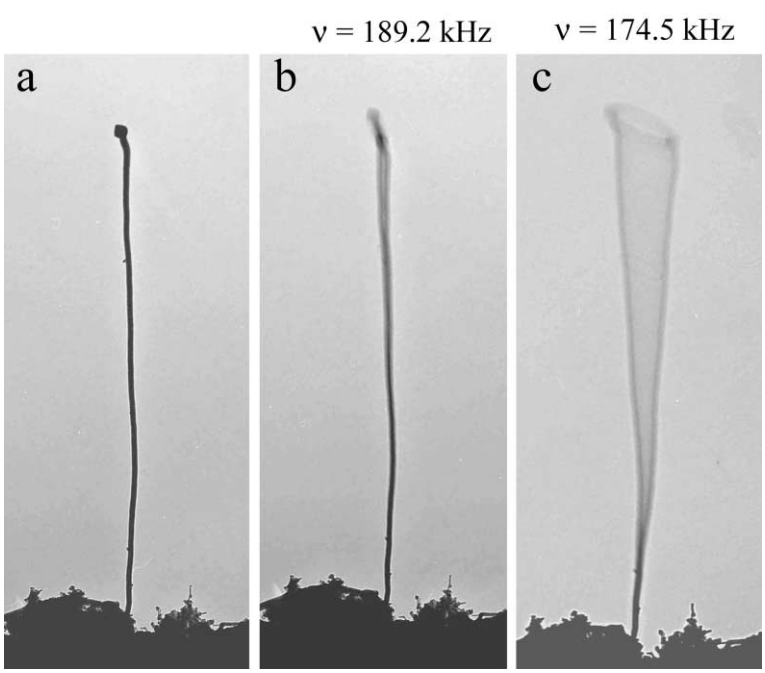

Fig. 4. A silica sheathed Si nanowire at (a) stationary and (b, c) resonance in different planes for the two slightly different resonance frequencies, showing the anisotropy effect.

Table 1
Bending modulus of carbon nanotubes produced by pyrolysis

Outer diameter D (nm) (± 1)	Inner diameter D_1 (nm) (± 1)	Length L (μm) (± 0.05)	Frequency f (MHz)	E_b (GPa)
33	18.8	5.5	0.658	32 ± 3.6
39	19.4	5.7	0.644	26.5 ± 3.1
39	13.8	5	0.791	26.3 ± 3.1
45.8	16.7	5.3	0.908	31.5 ± 3.5
50	27.1	4.6	1.420	32.1 ± 3.5
64	27.8	5.7	0.968	23 ± 2.7

2.2. Bending modulus of carbon nanotubes produced by pyrolysis

Carbon nanotubes produced by pyrolysis usually contain a high density of defects owing to the introduction of pentagonal and heptagonal carbon rings. To quantitatively determine the effect of growth defects on the bending modulus of carbon nanotubes, the mechanical properties of the aligned carbon nanotubes prepared by pyrolysis of iron(II) phthalocyanine were used [6]. The carbon nanotubes display the bamboo-like structure, which is very different from those produced by arc-discharge. If the structure of the carbon nanotubes can be approximated as a uniform tube structure, the bending modulus of the tube can be calculated using Eq. (1) from the experimentally measured resonance frequency, as summarized in Table 1. It is apparent that the bending modulus is much lower than those for the nanotubes of equivalent sizes produced by arc-discharge. The softening of the nanotubes produced by pyrolysis is attributed to defects, mainly point defects, present in the nanotubes [7].

Carbon nanotubes produced by pyrolysis usually have not only a high density of point defects but also volume defects. Fig. 5 shows a TEM image of a nanotube that exhibits a visible defect at points indicated by arrowheads. From the vibration shape of the nanotube, there is no abrupt change at the defect point and the vibration curve is smooth. If Eq. (1) is still applicable to this case, resonance measurement showed that the bending modulus of the nanotube is 2.2 GPa, about 15 times smaller than the nanotubes produced by arc-discharge.

To trace the effect of a volume defect on the mechanical properties, we have examined the electrostatic deflection of a nanotube when a constant voltage is applied across the electrodes (Fig. 6). The nanotube shows a smooth deflection without visible change in its shape near the volume defect. We did not observe an abrupt change in the nanotube shape at a defect point. Therefore, the volume defect seems do not introduce any significant softening at the local region due, most probably, to the collectively rippling deformation on the inner arc of the bent nanotube [7], and the vibration of the entire system could still be described by the elasticity theory.

2.3. Young's modulus of SiC–SiO_x composite nanowires

One-dimensional nanowires are ideal quantum structures for investigating size-dependent transport and electrical properties. Silicon carbide is a wide bandgap semiconducting material used for high-temperature, high-frequency, and high-power applications. Recently, Morales and Lieber [8], Lee et al. [9] and Yu et al. [10] have extrapolated on the ideas entailed in the vapor–liquid–solid (VLS) technique to develop the laser ablation of metal containing silicon targets as a means of obtaining bulk quantities of silicon nanowires. We have recently applied the elevated temperature synthesis to generate silicon carbide-silica composite nanowires [11]. The assynthesized materials are grouped into three basic nanowire structures: pure SiO_x nanowires, coaxially SiO_x sheated β-SiC nanowires, and

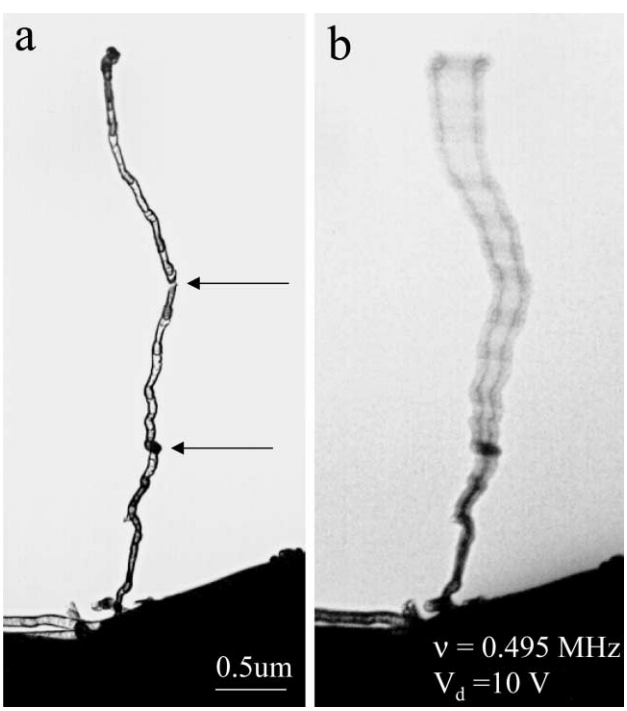

Fig. 5. A carbon nanotube produced by pyrolysis at (a) stationary and (b) the first harmonic resonance. The arrowheads indicate the presence of volume defects along the body of the nanotube.

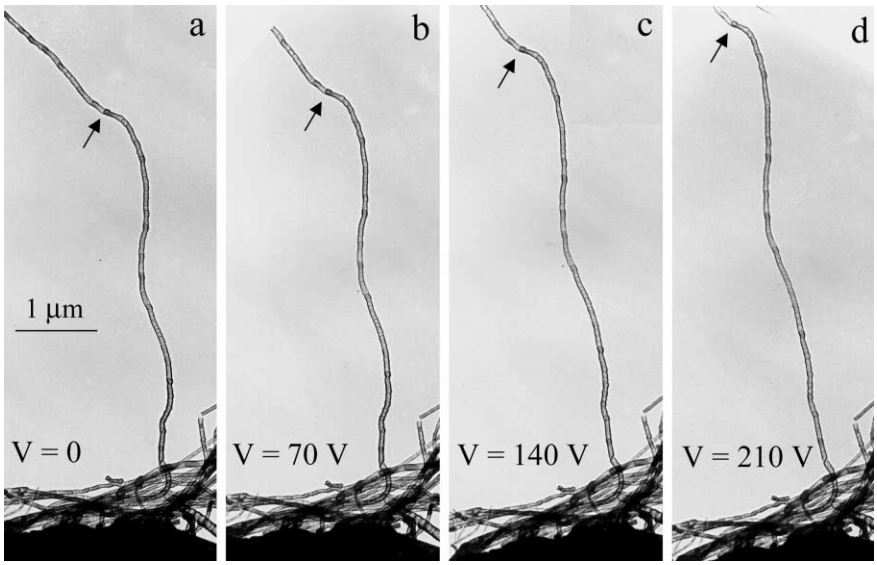

Fig. 6. Electrostatic defections of a carbon nanotube produced by pyrolysis under the applied DC voltage, showing no local softening at the site of a volume defect indicated by an arrowhead.

biaxial β-SiC–SiO_x nanowires [12]. The bending modulus was first measured for pure silica nanowires (Table 2). It can be seen that the data are fairly consistent, and we obtain a Young's modulus about half of that for large size silica fibers (18) (the Young's moduli of the fused silica fibers are: for $D = 102$ μm, $E = 72.3$ GPa; $D = 20$ μm, $E = 71.9$ GPa; $D = 4.1$–6.0 μm, $E = 56.3$ GPa).

Similarly, the bending modulus for coaxial SiC–SiO was measured (Table 3). The effective modulus of the composite nanowire increases as the diameter of the nanowire increases. Theoretically, the effective flexural rigidity of a composite coaxial nanowire is:

$$E_{\text{eff}} I_{\text{eff}} = E_{\text{Silica}} I_{\text{Silica}} + E_{\text{SiC}} I_{\text{SiC}},$$

where E is the Young's modulus of bulk material and I is the moment of inertia. Thus, the effective Young's modulus of the nanowire with cylindrical symmetry is given by $E_{\text{eff}} = \alpha E_{\text{SiC}} + (1-\alpha)E_{\text{Silica}}$, where $\alpha = (D_c/D_s)^4$, D_s and D_c are the outer and inner diameters of the SiO_x sheath, respectively. The theoretically expected Young's modulus is consistent with the experimentally measured values.

Table 2
Measured Young's modulus

D (nm) (±2 nm)	L (μm) (±0.2 μm)	f_o (MHz)	E (GPa)
42	11.7	0.160	31±5.1
53	6.3	0.562	20±4.0
58	3.8	1.950	27±7.5
70	13.0	0.200	26±3.1
95	14.8	0.232	32±3.1

E, for solid silica nanowires. E was calculated using the density of bulk amorphous SiO_2. f_o: the fundamental resonance frequency; L: nanowire length; D: nanowire diameter.

2.4. Electrostatic charges on carbon nanotubes

The unique structure of carbon nanotubes clearly indicates they are ideal objects that can be used for producing high field emission current density in flat panel display [13]. Most of the current measurements were made using a film of the aligned carbon nanotubes, in which there is a large variation in nanotube diameters and lengths, resulting in difficulty to clearly characterize the true switching-on field for electron field emission. Using the in situ TEM set-up we built, some of the interesting aspects of electron field emission from carbon nanotubes can be revealed. Fig. 7 shows a series TEM images of a carbon nanotube by selecting the electron deflected to different angular ranges around the central transmitted beam. The image contract reflects the potential distribution at and around the body of the nanotube, and it can be understood as follows. If the carbon nanotube is positively charged, electrons flying from both sides of the nanotube will be deflected electrostatically towards each other. In the diffraction plane, if a small size objective aperture is positioned slightly off the center, images shown in Fig. 7 can be produced simply by excluding the electrons deflected off the center transmitted beam in different directions. The dark contrast near the tips of the nanotube is directly associated with the projected potential field contributed by the charges on the tip of the nanotube. The nonuniform contrast adjacent to a defect clearly shows the build up of charges. Therefore, electrostatic charges accumulate not only at the tips, bodies of the nanotubes, but also at the defect sites. These observations

Table 3
Measured Young's modulus of coaxial cable structured SiC–SiO_x nanowires (SiC is the core, and silica is the sheath)

D_s (nm) ($\pm$2 nm)	D_c (nm) ($\pm$1 nm)	L (μm) ($\pm$0.2 μm)	f_o (MHz)	E_{eff} (GPa) (experimental)	E_{eff} (GPa) (theoretical (20))
51	12.5	6.8	0.693	46 $\pm$ 9.0	73
74	26	7.3	0.953	56 $\pm$ 9.2	78
83	33	7.2	1.044	52 $\pm$ 8.2	82
132	48	13.5	0.588	78 $\pm$ 7.0	79
190	105	19.0	0.419	81 $\pm$ 5.1	109

The densities of SiC and SiO_2 were taken from the bulk values ($\rho_{Silica} = 2.2 \times 10^3$ kg/m^3; $\rho_{SiC} = 3.2 \times 10^3$ kg/m^3).

are consistent with the expected results from electrodynamics to preserve the carbon nanotube, if conductive, as an equal potential body.

2.5. Electric field induced structural damage of carbon nanotubes

Under an externally applied electric field, carbon nanotubes can emit electrons. However, if the strength of the applied voltage exceeds a critical value to overcome the bonding energy of a carbon atom, structural damage could be generated as a result of splitting atoms off the tip. Our TEM set-up provides an ideal apparatus for directly observing this phenomenon. It is known that carbon nanotubes are comprised of concentric cylindrical graphitic sheets. Under a strong electric field, graphitic sheets are broken and pilled off (Fig. 8). This large-patch pilling process is different from the unraveling process proposed for interpreting the current fluctuation in electron field emission [14]. Here, we offer an alternative interpretation for the observed phenomenon. In fact, we have observed the vibration of nanotubes during electron emission, and the vibration is closely to be random and the vibration periodicity is a fraction of a second. This suggests that the electrons emitted from the tip come out ballistically as a

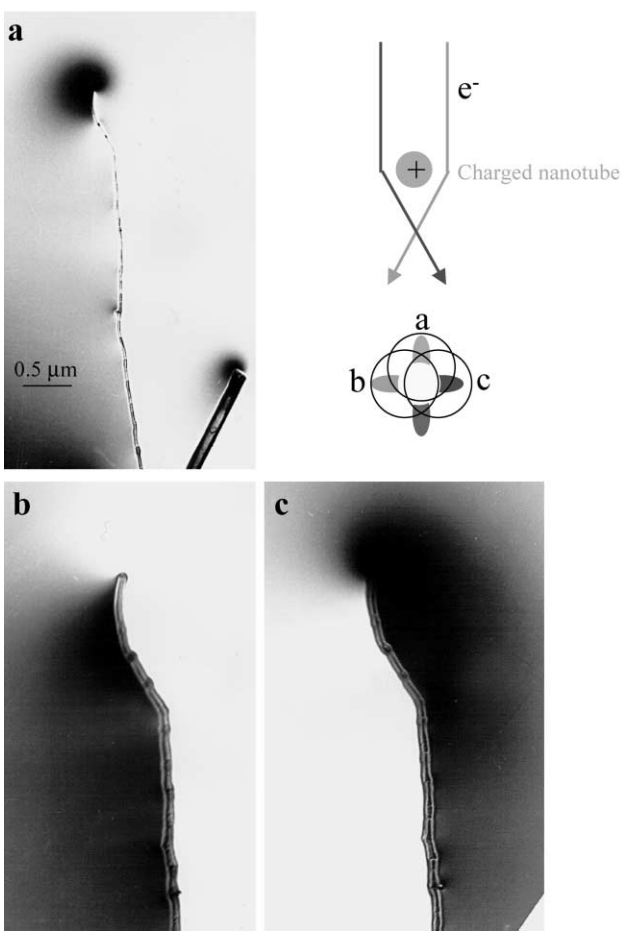

Fig. 7. TEM images recorded from a carbon nanotube under 100 V applied voltage by selecting the electrons deflected towards different direction using a small objective aperture. The positions of the objective aperture are schematically shown at the upper-right corner.

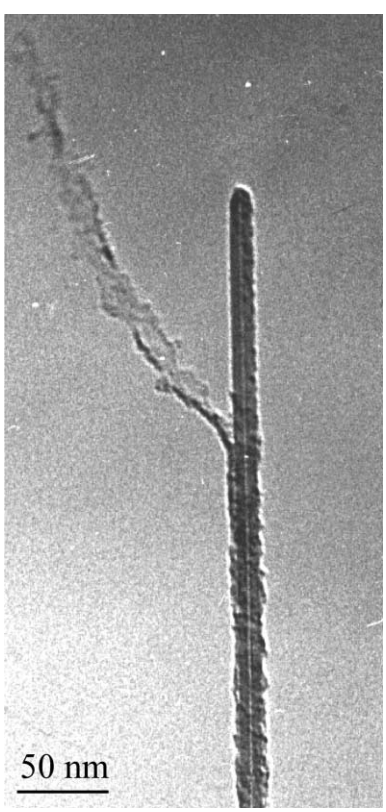

Fig. 8. In situ TEM observation the structural damage to a carbon nanotube induced by an electric field, showing the graphitic patch splitting effect.

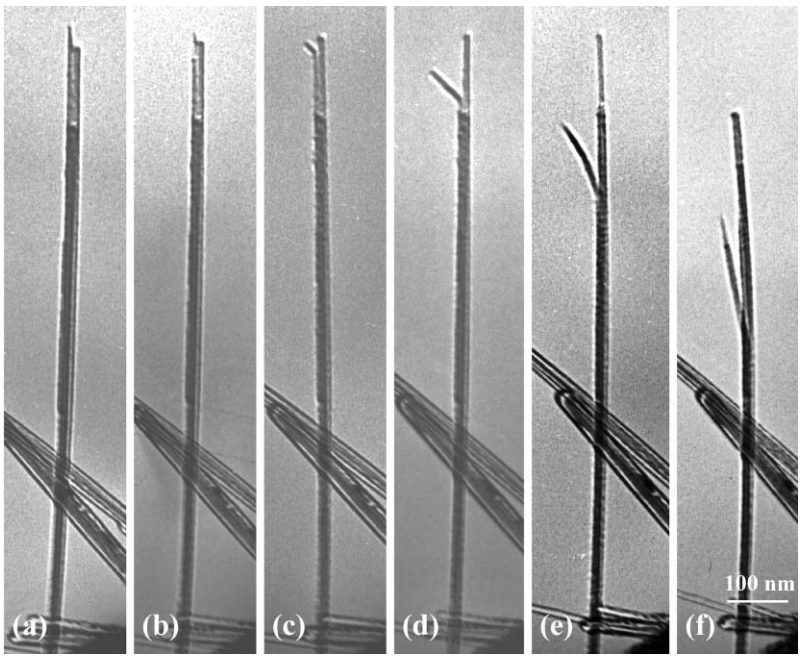

Fig. 9. A series of in situ TEM images showing the structural damage induced by an applied voltage, illustrating the splitting and segment breaking effect.

group rather than a continuous process. Therefore, there is a fluctuation in the charges accumulated at the tip, resulting in a vibration owing to a variation in the electrostatic force acting on the tip.

Shown in Fig. 9 is a series of TEM images recorded as the applied voltage increases from 80 to 150 V, showing the splitting, breaking and pilling off process at the tip of a carbon nanotube. The pilling of a carbon nanotube must involve the breaking of covalently bonded carbon–carbon chains, the strongest bonding in all of the known materials.

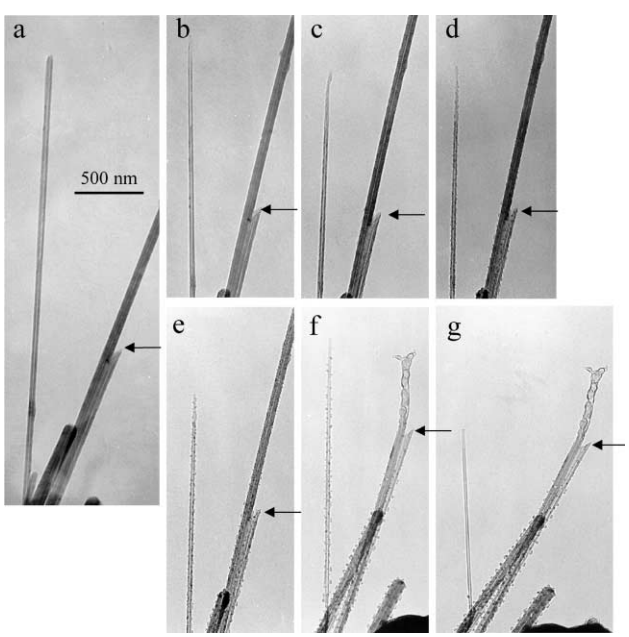

Fig. 10. A series of in situ TEM images showing the structural damage induced by an applied voltage, illustrating the stripping-off effect.

It is interesting to note that the graphitic cylindrical shells were scratched from the middle and came off as a whole piece (see Fig. 9), rather than a layer-by-layer stripping. This is a rather surprising result.

Fig. 10 shows a series of TEM images, illustrating the stripping off effect induced by an applied voltage. As the voltage increases, the outer layers of the carbon nanotubes were stripped off and became thinner. Simultaneously, their lengths are shortened. This observation clearly illustrates that the entire graphitic layers can be stripped off by an electrostatic field, resulting in sharper nanotubes. Further increase in the applied voltage results in the complete damage of the tube structure.

Using the same in situ TEM set-up, we have repeated the quantum conductance of multiwalled carbon nanotubes observed previously using an AFM apparatus [15]. It was confirmed that a clean and defect-free multiwalled carbon nanotubes gives ballistic transport. Surface contamination can destroy the quantum conductance [16].

3. Conclusions

The objective of this paper is to review the nano-scale manipulation and measurements carried out using an in situ TEM. The approaches demonstrated here are unique applications for measurements the electrical, mechanical and field emission properties of wire-like nanomaterials. In this technique, the properties measured from a single carbon nanotube can be directly correlated with the intrinsic atomic-scale microstructure of the nanotube, providing a one-to-one correspondence in property–structure relationship. We strongly believe that TEM can be powerful for

characterizing nanomaterials in not only their structures, but also intrinsic properties. Its manifold applications remain to be discovered.

Acknowledgements

Thanks to Professor J.L. Gole and Mr. J.D. Scout for providing the SiC nanowire specimens and Dr. Liming Dai for the carbon nanotube specimens. RPG thanks the partial support from China NSF. Thanks for the financial support of NSF Grants DMR-9971412 and DMR-9733160. Thanks to the Georgia Tech Electron Microscopy Center for providing the research facility.

References

[1] Z.L. Wang (Ed.), Characterization of Nanophase Materials. Wiley-VCH, New York, 1999, pp. 1–400.
[2] P. Poncharal, Z.L. Wang, D. Ugarte, W.A. de Heer, Science 283 (1999) 1516.
[3] Z.L. Wang, P. Poncharal, W.A. de Heer, Microsc. Microanal. 6 (2000) 224.
[4] Z.L. Wang, P. Poncharal, W.A. de Heer, Pure Appl. Chem. 72 (1–2) (2000) 209.
[5] L. Meirovich, Element of Vibration Analysis. McGraw-Hill, New York, 1986.
[6] S.M. Huang, L.M. Dai, A.W.H. Mau, J. Phys. Chem. B 103 (1999) 4223.
[7] R.P. Gao, Z.L. Wang, Z.G. Bai, W. de Heer, L. Dai, M. Gao, Phys. Rev. Letts. 85 (2000) 622.
[8] A.M. Morales, C.M. Lieber, Science 279 (1998) 208.
[9] S.T. Lee, N. Wang, Y.F. Zahng, Y.H. Tang, MRS Bull. 36 (1999) August.
[10] D.P. Yu, Z.G. Bai, Y. Ding, Q.L. Hang, H.Z. Zhang, J.J. Wang, Y.H. Zou, W. Qian, G.C. Xiong, H.T. Zhou, S.Q. Feng, Appl. Phys. Lett. 72 (1998) 3458.
[11] J.L. Gole, J.D. Scout, W.L. Rauch, Z.L. Wang, Appl. Phys. Lett. 76 (2000) 2346.
[12] Z.L. Wang, Z.R. Dai, Z.G. Bai, R.P. Gao, J. Gole, Appl. Phys. Letts. 77 (2000) 3349.
[13] W.A. de Heer, A. Chatelain, D. Ugarte, Science 268 (1995) 845.
[14] A.G. Rinzler, J.H. Hafner, P. Nikolaev, L. Lou, S.G. Kim, D. Tomanek, P. Nordlander, D.T. Colbert, R.E. Smalley, Science 269 (1995) 1550.
[15] S. Frank, P. Poncharal, Z.L. Wang, W.A. de Heer, Science 280 (1998) 1744.
[16] Z.L. Wang, P. Poncharal, P. Keghelian, W.A. de Heer, Phys. Rev. Lett. (2001) submitted for publication.